Impaired Inactivation of L-Type Ca^{2+} Current as a Potential Mechanism for Variable Arrhythmogenic Liability of HERG K$^+$ Channel Blocking Drugs

Jae Gon Kim[1,2‡], Dong Jun Sung[4‡], Hyun-ji Kim[1‡], Sang Woong Park[5], Kyung Jong Won[5], Bokyung Kim[5], Ho Chul Shin[6], Ki-Suk Kim[2,3], Chae Hun Leem[7], Yin Hua Zhang[8], Hana Cho[1]*, Young Min Bae[5]*

1 Department of Physiology and the Samsung Biomedical Research Institute, Sungkyunkwan University School of Medicine, Suwon, South Korea, 2 Next-Generation Pharmaceutical Research Center, Korea Institute of Toxicology, Korea Research Institute of Chemical Technology, Daejeon, South Korea, 3 Human and Environmental Toxicology Program, University of Science and Technology, Daejeon, South Korea, 4 Division of Sport Science, College of Science and Technology, Konkuk University, Choongju, South Korea, 5 Department of Physiology, KU Open Innovation Center, Research Institute of Medical Science, Konkuk University School of Medicine, Chungju, South Korea, 6 Department of Veterinary Pharmacology and Toxicology, College of Veterinary Medicine, Konkuk University, Seoul, South Korea, 7 Department of Physiology, University of Ulsan College of Medicine, Seoul, South Korea, 8 Department of Physiology, Seoul National University College of Medicine, Seoul, South Korea

‡ These authors are joint co-first authors on this work.
* hanacho@skku.edu; ymbae30@kku.ac.kr

Abstract

The proarrhythmic effects of new drugs have been assessed by measuring rapidly activating delayed-rectifier K$^+$ current (I_{Kr}) antagonist potency. However, recent data suggest that even drugs thought to be highly specific I_{Kr} blockers can be arrhythmogenic via a separate, time-dependent pathway such as late Na$^+$ current augmentation. Here, we report a mechanism for a quinolone antibiotic, sparfloxacin-induced action potential duration (APD) prolongation that involves increase in late L-type Ca^{2+} current (I_{CaL}) caused by a decrease in Ca^{2+}-dependent inactivation (CDI). Acute exposure to sparfloxacin, an I_{Kr} blocker with prolongation of QT interval and torsades de pointes (TdP) produced a significant APD prolongation in rat ventricular myocytes, which lack I_{Kr} due to E4031 pretreatment. Sparfloxacin reduced peak I_{CaL} but increased late I_{CaL} by slowing its inactivation. In contrast, ketoconazole, an I_{Kr} blocker without prolongation of QT interval and TdP produced reduction of both peak and late I_{CaL}, suggesting the role of increased late I_{CaL} in arrhythmogenic effect. Further analysis showed that sparfloxacin reduced CDI. Consistently, replacement of extracellular Ca^{2+} with Ba^{2+} abolished the sparfloxacin effects on I_{CaL}. In addition, sparfloxacin modulated I_{CaL} in a use-dependent manner. Cardiomyocytes from adult mouse, which is lack of native I_{Kr}, demonstrated similar increase in late I_{CaL} and afterdepolarizations. The present findings show that sparfloxacin can prolong APD by augmenting late I_{CaL}. Thus, drugs that cause delayed I_{CaL} inactivation and I_{Kr} blockage may have more adverse effects than those that selectively block I_{Kr}. This mechanism may explain the

Abbreviations: AP, action potential; APD, action potential duration; CDI, Ca^{2+}-dependent inactivation; EAD, early afterdepolarization; hERG, human *Ether-à-go-go*-related gene; I_{CaL}, L-type Ca^{2+} current; I_{CaT}, T-type Ca^{2+} current; I_{Kr}, rapidly activating delayed-rectifier K$^+$ current; LQT, long QT; SPX, sparfloxacin; TdP, Torsade de Pointes; VT, ventricular tachycardia; VDI, voltage-dependent inactivation.

reason for discrepancies between clinically reported proarrhythmic effects and I_{Kr} antagonist potencies.

Introduction

Drug-induced QT interval prolongation and the appearance of torsade de pointes (TdPs) are recognized as potential risks associated with the use of a wide range of noncardiovascular drugs including antibiotics [1–4]. Quinolone antibiotics have been suggested to have a class effect of blocking the human *Ether-a-go-go*-related gene (hERG) K$^+$ channel expressing the rapid component of the delayed rectifier current (I_{Kr}) in the human heart, and thus prolong action potential duration (APD), which is associated with QT interval prolongation. The quinolone antibiotic sparfloxacin (SPX) has been withdrawn from U.S. drug market, because it was shown to induce QT interval prolongation and ventricular arrhythmia [5, 6]. Another quinolone, grepafloxacin, was withdrawn because it induced TdP, a polymorphic ventricular tachycardia (VT) linked to excessive QT interval prolongation [7]. Concern over the proarrhythmic effects of many other quinolone antibiotics continues to grow. In nonclinical studies, the proarrhythmic effects of clinically used quinolone antibiotics have been assessed by measuring their associated I_{Kr} antagonist potency. However, discrepancies between clinically reported proarrhythmic effects and in vitro observations exist. For example, the antibiotic moxifloxacin blocks I_{Kr} but has been associated with drug-induced long QT syndrome (LQT) only very rarely [8, 9].

Cardiac rhythm and contractility are regulated by the composite functions of cardiac myocyte ion channels. Specifically, the lengthening and flattening of action potential (AP) plateaus are determined by the sum of inward and outward currents. I_{CaL} contribute to inward currents, maintaining the plateau phase of ventricular AP (phase 2). Inhibition of I_{CaL} shortens the AP, whereas inhibition of outward I_{Kr} results in AP prolongation. Therefore, if both K$^+$ and Ca^{2+} channels are inhibited, I_{CaL} inhibition may counteract the I_{Kr}-blocking effects of quinolone antibiotics. Indeed, Xu *et al.*(2003) reported that drugs with dual blocking action against hERG K$^+$ and Ca^{2+} channels are less likely to cause arrhythmias than drugs with selective blocking activity against hERG K$^+$ current [10]. On the other hand, enhancing I_{CaL} while blocking I_{Kr} may aggravate APD prolongation and/or generate early afterdepolarization (EAD) upstrokes.

During a normal AP, I_{CaL} peaks early, triggering robust sarcoplasmic reticulum Ca^{2+} release before partially inactivating due to two processes: Ca^{2+}-dependent inactivation (CDI), mediated by Ca^{2+} binding to calmodulin (CaM) tethered to the C-terminus of the channel, and voltage-dependent inactivation (VDI). The rate and degree of I_{CaL} inactivation due to these processes during the late phase of the APD has a major effect on repolarization. This raises the possibility that instead of potentiating I_{CaL}, modifying its shape by altering its inactivation kinetics might lead to APD prolongation and EAD. In a recent study, elimination of CDI in guinea pig ventricular myocytes via expression of Ca^{2+}-insensitive CaM (CaM1234) was shown to produce "ultralong" Aps [11].

In the present study, we sought to determine the relevance of I_{CaL} in APD prolongation effects of SPX. We analyzed the biophysical properties of L-type Ca^{2+} channels affecting APD. SPX reduced peak I_{CaL}. However this quinolone antibiotic augmented late I_{CaL} by attenuating CDI, which promoted APD prolongation in cardiac myocytes. In contrast, I_{Kr} blockers not associated with serious arrhythmias—ketoconazole, ciprofloxacin, enoxacin, ofloxacin, and levofloxacin produced no change in I_{CaL} or decreased both peak and late I_{CaL}, suggesting the role of increased late I_{CaL} in arrhythmogenic effect. Our results suggest an importance of calcium channel inactivation in producing the arrhythmogenic effects of SPX and, as such, it is

necessary to consider I_{CaL} property changes when assessing drugs for QT prolonging and arrhythmogenic liability.

Materials and Methods

Cardiomyocyte isolation and culture

All animal care and experimental procedures complied with the National Institutes of Health guidelines, and the Institutional Animal Care and Use Committee of Konkuk University and Sungkyunkwan University approved this study. Neonatal ventricular myocytes were isolated from 1 to 2-day-old Sprague-Dawley (SD) rats (Nara Biotech, Seoul, Korea) by using a previously reported method [12]. Ventricular regions of neonatal rat hearts were excised (approximately, the lower third) and the tissues (approximately 1–2 mm) were minced on ice. The minced tissues were treated with a solution containing 0.1% collagenase (Wako, Japan), 0.1% trypsin, and 1% glucose in phosphate-buffered saline (Ca^{2+}/Mg^{2+}-free) at 37°C for 10 min. After the supernatant from the first digestion was removed, three 10-min digestions were performed using the same enzyme solution. The supernatants were stored in DMEM/F-12 culture medium containing 10% fetal bovine serum, 5% horse serum, penicillin-streptomycin (100 U/ml and 100 µg/ml, respectively) in a 4°C ice chamber and the centrifuged for 7 min at $700 \times g$. The cell pellets were incubated at 37°C in a 95% O$_2$ incubator for 1.5 h to attach non-cardiac myocytes to microscope cover glass. The cells were subsequently cultured on the cover glass for 3 days at 37°C and 95% O$_2$. Cells cultured for 3–5 days were used for I_{CaL} current recordings.

Ventricular myocytes from adult mice (> 5 months) or 2-week-old SD rats were isolated as previously described with minor modifications [13]. Briefly, ventricular myocytes were isolated by perfusing Ca^{2+}-free NT solution containing collagenase (1 mg/ml, 4176, Worthington) and DL-dithiothreitol (1 mg/ml, D-0632, Sigma, St. Louis, MO, USA) through Langendorff columns at 37°C.

Electrophysiological recording

Cardiac myocytes were subjected to patch-clamp experiments. Whole-cell Ca^{2+} and Ba^{2+} currents were recorded using a conventional whole-cell patch-clamp configuration, outfitted with an EPC 8 patch-clamp amplifier (Heka, Germany). Voltage pulse generation was controlled using R-clamp software (R-clamp; provided by Dr. S.Y. Ryu). The data were digitized using the R-clamp software at a sampling rate of 5 kHz, after being low-pass filtered at 1 kHz. The patch pipettes were created from borosilicate glass capillaries (Clark Electromedical Instruments, Pangbourne, UK) by using a puller (PP-83; Narishige, Japan). Patch pipettes producing resistances of 1.5–2.5 MΩ in bathing solution were used. All experiments were performed at room temperature (20–25°C).

APs were recorded using a nystatin-perforated patch-clamp configuration, with an EPC10 patch-clamp amplifier (Heka, Germany). Data were digitized and current injection (125–175 pA, 9 ms) for AP generation were both controlled using Patch-Master software.

Solutions and Drugs

To record I_{CaL} in cardiac myocytes, NMDG-Tyrode's [143 mM N-methyl-D-glucamine (NMDG)-Cl, 5.4 mM CsCl, 0.33 mM NaH$_2$PO$_4$, 5 mM HEPES, 0.5 mM MgCl$_2$, 1.8 mM CaCl$_2$, 11 mM D-glucose, pH adjusted to 7.4 with HCl] was used as the bathing solution. The pipette solution contained 115 mM CsCl, 5 mM Mg-ATP, 10 mM HEPES, 5 mM ethylene glycol-bis (2-aminoethylether)-N,N,N,N,-tetraacetic acid (EGTA), and 5 mM creatine phosphate (disodium salt). The pH was adjusted to 7.3 by using CsOH. APs were recorded from single isolated

myocytes in a perforated patch configuration by using nystatin (200 µg/ml). Normal Tyrode's solution (143 mM NaCl, 5.4 mM KCl, 0.33 mM NaH$_2$PO$_4$, 5 mM HEPES, 0.5 mM MgCl$_2$, 1.8 mM CaCl$_2$, 11 mM D-glucose, pH adjusted to 7.4 with NaOH) was used as the bathing solution. The pipette solution for recoding APs contained 140 mM KCl, 10 mM HEPES, 5 mM EGTA, and 1 mM MgCl$_2$, and the pH was adjusted to 7.2 with KOH.

To record I$_{Na}$ in cardiac myocytes, 140 mM NaCl, 5 mM CsCl, 1.8 mM CaCl$_2$, 1 mM MgCl$_2$, 11 mM Glucose, 10 mM HEPES adjusted with NaOH (pH 7.4) was used as the bath solution. Nifedipine (1 µM), SN-6 (10 µM), and CdCl$_2$ (100 µM) were used to block L-type Ca^{2+} currents, NCX currents, and T-type Ca^{2+} currents, respectively. The pipette solution contained 20 mM CsCl, 100 mM Cs-Asp, 10 mM EGTA, 10 mM HEPES, 20 mM TEA-Cl, 5 mM Mg-ATP adjusted to 7.25 with CsOH.

Unless otherwise stated, all chemicals and drugs were purchased from Sigma-Aldrich; SPX (Fluca, 56968) and E4031 (Sigma, M5060) were prepared as stock solutions in dimethyl sulfoxide. The drugs were diluted in the bathing solution on the day of the experiment.

Statistical analysis

The results are shown as mean ± standard error of the mean. Student's *t*-tests or Fisher's exact test were performed to test for significance as appropriate using SigmaPlot. P values <0.05 were deemed to be statistically significant.

Results

SPX induces APD prolongation in the presence of I_{Kr} blocker

To test the hypothesis that factors other than I_{Kr} modulation play important roles in SPX-induced APD prolongation, the effects of SPX applied at concentrations between 10 and 300 µM were investigated in 2-week-old rat ventricular myocytes in the presence of E4031, a selective I_{Kr} blocker. APs were elicited by electrical stimulations delivered using a patch pipette in current clamp mode, at a stimulation frequency of 2 Hz. As shown in Fig 1A, 30 µM SPX significantly prolonged APD in the presence of 1 µM E4031. The time required for 90% repolarization (APD$_{90}$), increased from 54.5 ± 3.3 to 95.0 ± 13.6 ms after 10 min of 30-µM SPX treatment (paired *t*-test; n = 7, P < 0.05).

No changes in resting membrane potential (RMP) or in AP overshoot potentials were observed during SPX treatments. The mean RMP and overshoot potential values after SPX treatment were −68.5 mV (n = 7; P > 0.05 vs. −70.8 mV in the absence of SPX) and 53.5 mV (n = 7; P > 0.05 vs. 52.7 mV in the absence of SPX), respectively. The steady-state APD$_{90}$ values obtained at various SPX concentrations are summarized in Fig 1B. These data indicate that SPX-induced APD prolongation is not only attributable to blocking I_{Kr}, but is also influenced by additional channel modulation.

Effects of SPX on I_{CaL}

We next examined whether SPX enhances I_{CaL} in neonatal cardiomyocytes. By holding E$_m$ at −50 mV, we could successfully isolate I_{CaL} from I_{CaT} measurements (S1 Fig). Therefore, we used holding potential of −50 mV for all voltage-clamp experiments, excluding those reported in Fig 2, in which we applied a double pulse at −40 mV followed by 0 mV from a holding potential of −80 mV [14]. To eliminate voltage-gated K$^+$ currents and Na$^+$ currents, a Cs$^+$-rich pipette solution and Na$^+$-free (substituted with NMDG$^+$) bath solution was used. Fig 2A shows representative I_{CaL} measurements under control conditions and in the presence of 300 µM SPX, recorded from the same ventricular myocytes. The amplitude of the peak I_{CaL} was
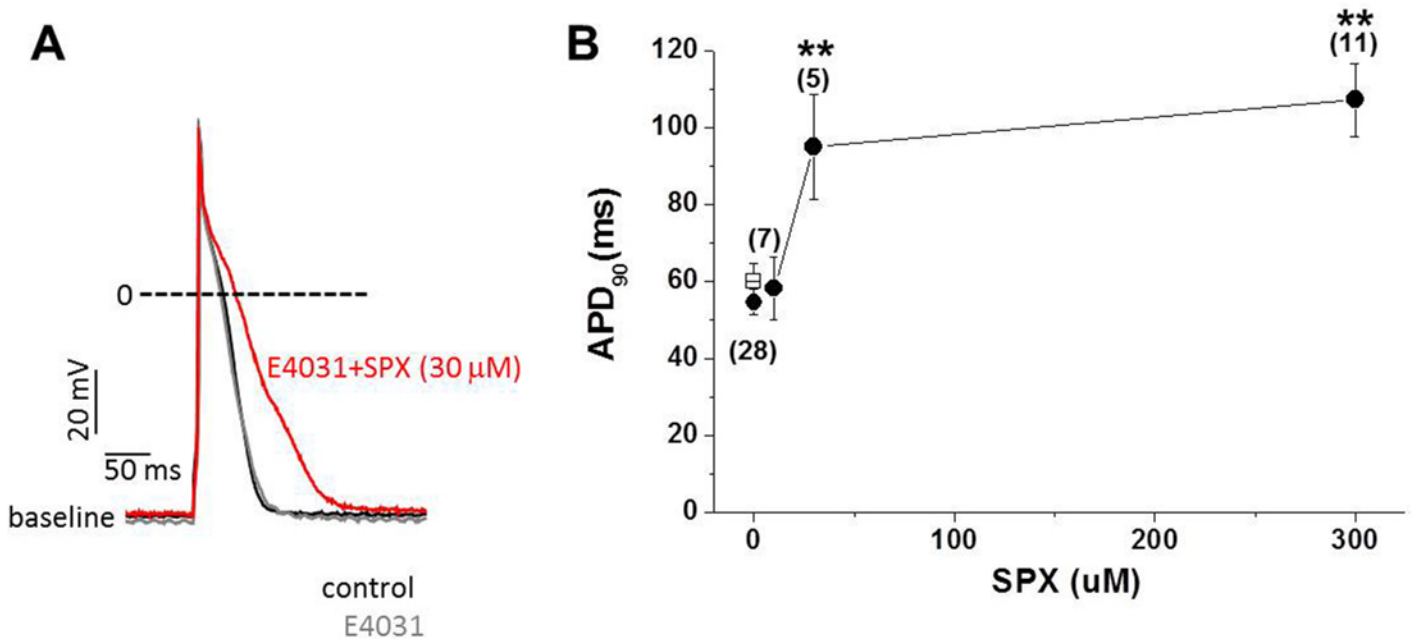
Fig 1. The effect of SPX on APs recorded in the presence of E4031. Action potentials were recorded by pacing myocytes at 2 Hz. In the presence of 10 μM E4031, SPX (10–300 μM) was applied. Data were obtained at 37°C by using the perforated patch technique. A, Examples of action potentials recorded before (gray) and after (red) SPX exposure at a concentration of 30 μM. The control action potential (black) before E-4031 treatment was also overlaid for comparison. B, APD_{90} was plotted as a function of SPX concentration. Asterisks indicate statistical significance (paired t-test; *P < 0.05, **P < 0.01). Error bars indicate standard error. The numbers in parentheses indicate the number of cells tested.

doi:10.1371/journal.pone.0149198.g001

reduced after SPX treatment. The I–V curves indicated that the peak I_{CaL} was decreased after 300 μM SPX treatment at all potentials ranging from −40 to +50 mV, without altering the I–V relationship (n = 10; Fig 2B). Inactivation, however, was slowed by SPX treatment. Slower I_{CaL} decay values resulted in larger current amplitudes in the presence of SPX at the end of the 200 ms pulse (Fig 2C). The amplitude of this current was larger over the voltage range 0 to +20 mV —i.e. the range in which the AP plateau typically occurs.

We also examined the effects on I_{CaL} of multiple I_{Kr} blockers that have not been associated with severe arrhythmias. Ciprofloxacin, enoxacin, ofloxacin, and levofloxacin are quinolone antibiotics with variable I_{Kr} potencies that are rarely associated with LQTS risk [15, 16]. They had no effect on I_{CaL} (S2 Fig). We also examined the effect on I_{CaL} of ketoconazole an antifungal agent which is known to block I_{Kr} but is not associated with TdP risk [17, 18]. Ketoconazole did decrease I_{CaL} (Fig 2D). In contrast to SPX, however, it reduced late I_{CaL} as well as peak I_{CaL} (Fig 2E). Taken together, these data suggest that SPX increased late I_{CaL} that might be related with its ability to induce arrhythmias.

Effect of SPX on the Inactivation Kinetics of I_{CaL}

To further investigate the effect of SPX on inactivation kinetics, the decay phase of I_{CaL} was fitted using an exponential function. When the decay phase was fitted using a monoexponential function, the time constant (τ) was significantly increased by SPX treatment (Fig 3A). The voltage dependence of τ remained unchanged in the presence of SPX. As shown in Fig 3B, the effects of SPX on inactivation kinetics were dose-dependent. Taken together, these results suggest that SPX induces APD prolongation by slowing I_{CaL} inactivation.
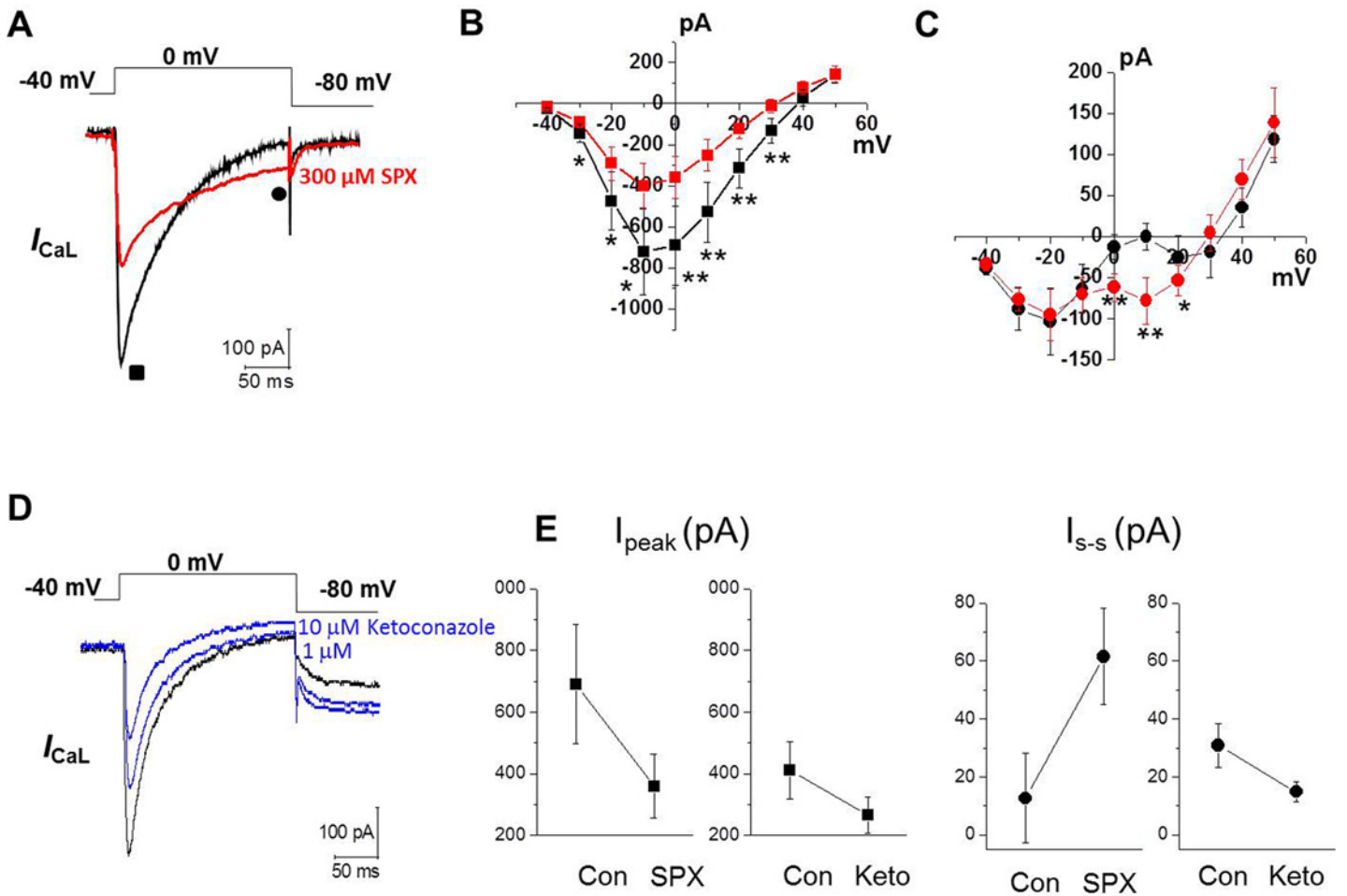
Fig 2. Effect of SPX on I_{CaL}. A, Representative traces of I_{CaL} during a 200-ms voltage-clamp pulse from −40 to 0 mV before (black) and after (red) exposure to 300 μM SPX. B–C, current–voltage (I-V) relationships of I_{peak} (■, B) and $I_{end\ of\ pulse}$ (●, C) under control conditions (black) and after application of 300 μM SPX (red) (n = 10). D, Representative traces of I_{CaL} to 1 μM and 10 μM of ketoconazole (blue) (n = 4). E, The comparison of I_{peak} (■, left) and I_{s-s} (●, right) from I_{CaL} before and after 300 μM SPX (n = 10) or 10 μM ketoconazole (n = 4). *P < 0.05 **P < 0.01.

SPX reduces Ca²⁺-dependent I_{CaL} inactivation

The effects of SPX on late I_{CaL} inactivation were investigated using conventional double-pulse protocol. Prepulses 1000 ms in duration and at various potentials ranging from −50 to +50 mV in 10 mV steps preceded a 100-ms test pulse at 0 mV. The superimposed current responses to the test pulse (0 mV) are shown in Fig 4A (left, control; right, 300 μM SPX). The slow inactivating I_{CaL} in the presence of SPX indicates that SPX exerts a pharmacological effect (Fig 4A, right).

Under control conditions, inactivation increased sharply as the prepotential increased from −40 to −20 mV, reaching a maximum of ~95.8% at +10 mV (Fig 4B). At prepulse potentials greater than +20 mV, the extent of inactivation decreased, resulting in a U-shaped $I_{Ca,L}$ inactivation curve. The data from −100 to +10 mV were fitted using the following Boltzmann equation:

$$y = (A_1 - A_2) / \left\{ 1 + \exp\left[\frac{(V - V_{1/2})}{\kappa} \right] \right\} + A_2$$
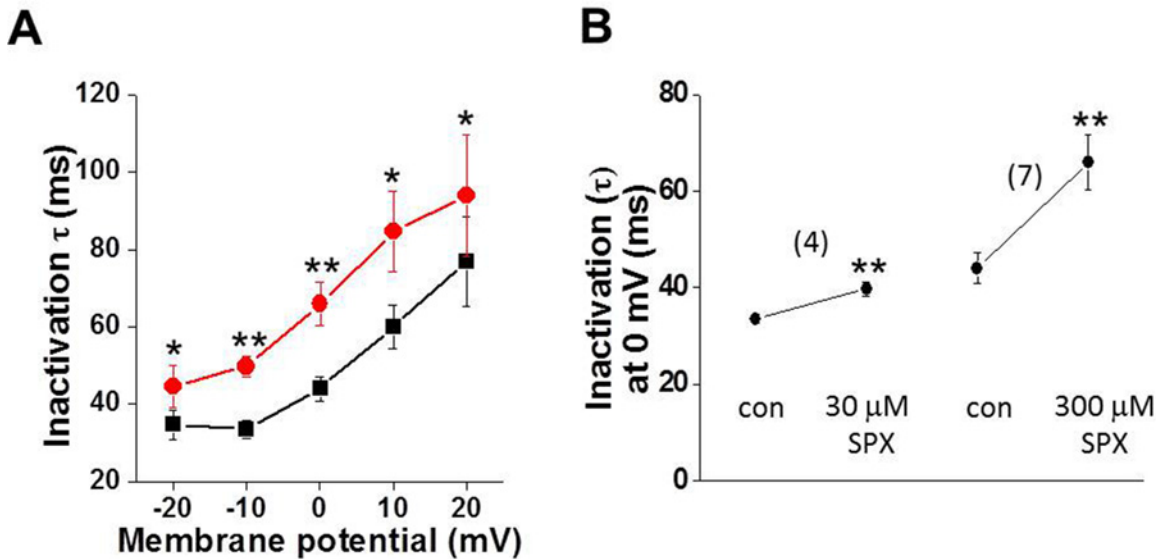
Fig 3. Effects of SPX on I_{CaL} inactivation time course. A, Summary of the effects of SPX (300 μM) on the time course (time constants, τ) of inactivation at various membrane potentials (n = 4–5). B, Summary of the concentration-dependent slowing of I_{CaL} inactivation by SPX at 0 mV (n = 4–5). *P < 0.05 **P < 0.01.

doi:10.1371/journal.pone.0149198.g003

where V is the membrane potential, $V_{1/2}$ is the membrane potential of half-maximum inactivation, and k is the slope of the inactivation curve. A_1 represents the maximal amplitude and A_2 is the amplitude of the non-inactivating component of $I_{Ca,L}$. $V_{1/2}$ was −26.2 ± 1.4 mV and k was +4.9 ± 0.7 mV under control condition.

The current availability curves produced in the presence of SPX (Fig 4B) indicate that SPX significantly reduced steady-state inactivation. When the data from −100 to +10 mV were fitted using the Boltzmann equation, the A_2 value, the amplitude of the non-inactivating component of $I_{Ca,L}$, was increased by SPX (0.087 ± 0.008 vs. 0.042 ± 0.012 in control, n = 5, P < 0.01). Neither $V_{1/2}$ nor k were affected (-26.6 ± 1.5 mV and +4.8 ± 0.8 mV, respectively; P > 0.05). In addition, at prepulse potentials greater than 0 mV, I_{CaL} amplitudes in the presence of SPX were greater than those under control conditions (P < 0.01; paired t-test; n = 5).

We confirmed that no differences in the steady-state activation curves (Fig 4C) were present before and after SPX treatment. The voltages for half-activation were −22.2 ± 0.1 mV (n = 10) in the control and −23.2 ± 1.2 mV (n = 10) in the presence of SPX (paired t-test, P > 0.05). These data suggest that SPX attenuates inactivation, leading to slower I_{CaL} decay.

L-type Ca²⁺ channels can be inactivated by two different mechanisms: CDI and VDI. The Ca²⁺-dependent aspect of L-type Ca²⁺ channel inactivation is dependent on Ca²⁺ entry. Therefore, essentially all inactivation of Ba²⁺ current through the L-type Ca²⁺ channels is voltage dependent. The substitution of Ba²⁺ ions for Ca²⁺ has been used widely to separate the contribution VDI from CDI to the macroscopic I_{CaL}. We confirmed the results reported previously, showing the Ca²⁺ dependence of CDI in our cells and that the effects of SPX are changed by replacing Ca²⁺ with Ba²⁺ (Fig 5). As shown in Fig 5A, SPX did not slow Ba²⁺ current inactivation. SPX did not increase the inactivation time constant, but instead reduced it, indicating that the attenuation of I_{CaL} inactivation by SPX was abolished (Fig 5B). In addition, SPX had little effect on the steady-state inactivation of Ba²⁺ currents (Fig 5C). These results confirm that SPX specifically modulates CDI.
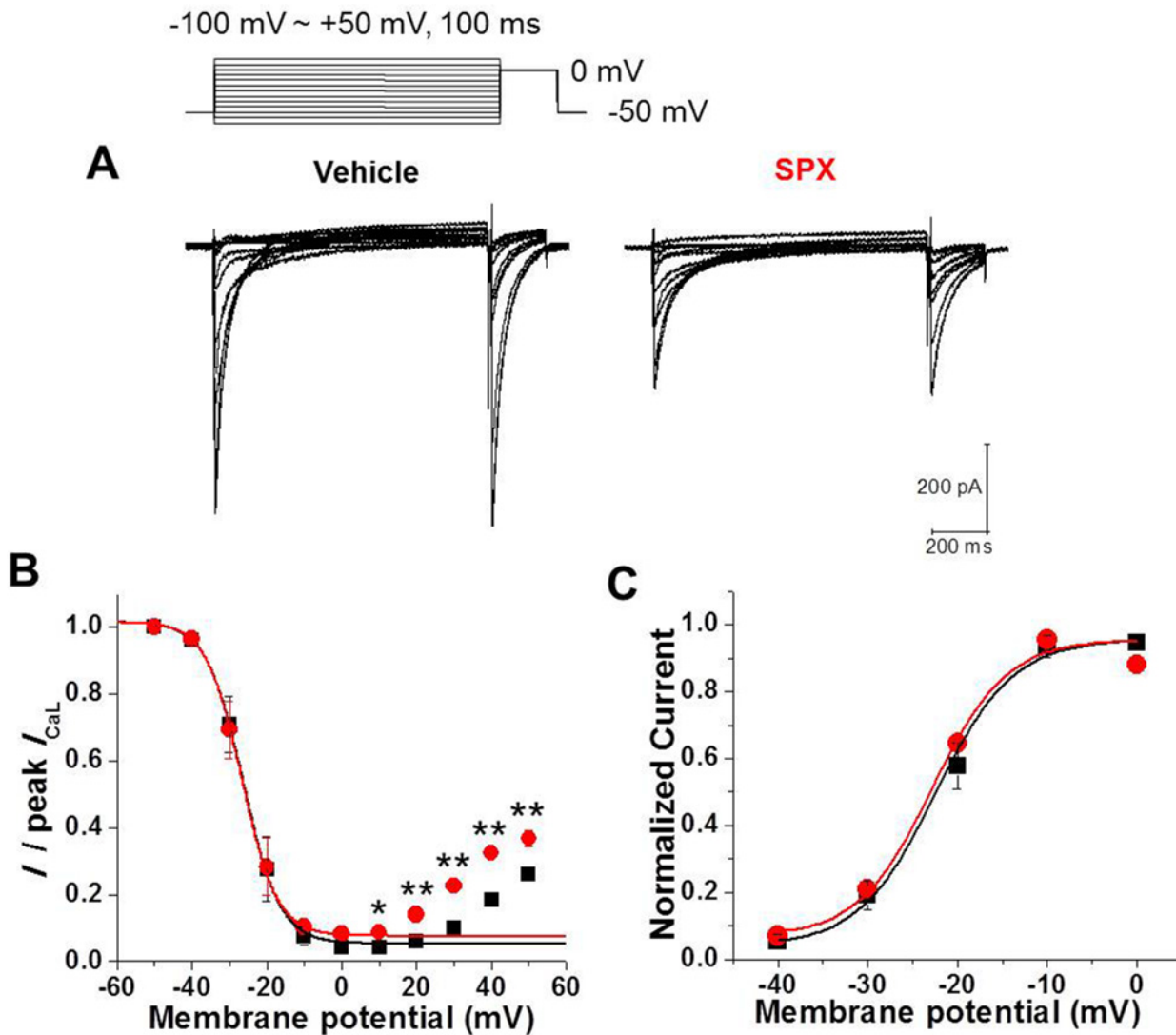
Fig 4. Effect of SPX on the steady-state inactivation of I_{CaL}. A, The steady-state inactivation levels were measured by using double-pulse protocol. B, Steady-state inactivation curves for the I_{CaL} in the absence and presence of SPX (300 μM). C, Voltage dependence of I_{CaL} activation in the absence and presence of SPX (300 μM). The half-activation voltage was not significantly changed by SPX (n = 10, paired t-test, P > 0.05).

Use-dependency

Since SPX slowed the inactivation of I_{CaL} by inhibiting CDI, it is expected that repetitive application of depolarizing voltage steps may cause less accumulation of I_{CaL} inactivation in the presence of SPX. In order to prove this hypothesis, a series of depolarizing step pulses at frequencies of 2Hz were applied (Fig 6A, inset). Fig 6A and 6B shows superimposed current traces of cells in the absence and presence of SPX, respectively. When the depolarizing step pulses were applied repetitively under control conditions, the I_{CaL} peak amplitudes were gradually decreased (50.6 ± 7.3% of the initial level at pulse 13; Fig 6C). In the presence of SPX (300 μM), however, this gradual decrease was significantly attenuated, with the I_{CaL} peak amplitude being 63.3 ± 5.7% of the initial level by pulse 13 (Fig 6C). Fig 6C illustrates the gradual decrease of I_{CaL} peak amplitudes during repetitive pulses in the absence and presence of SPX.
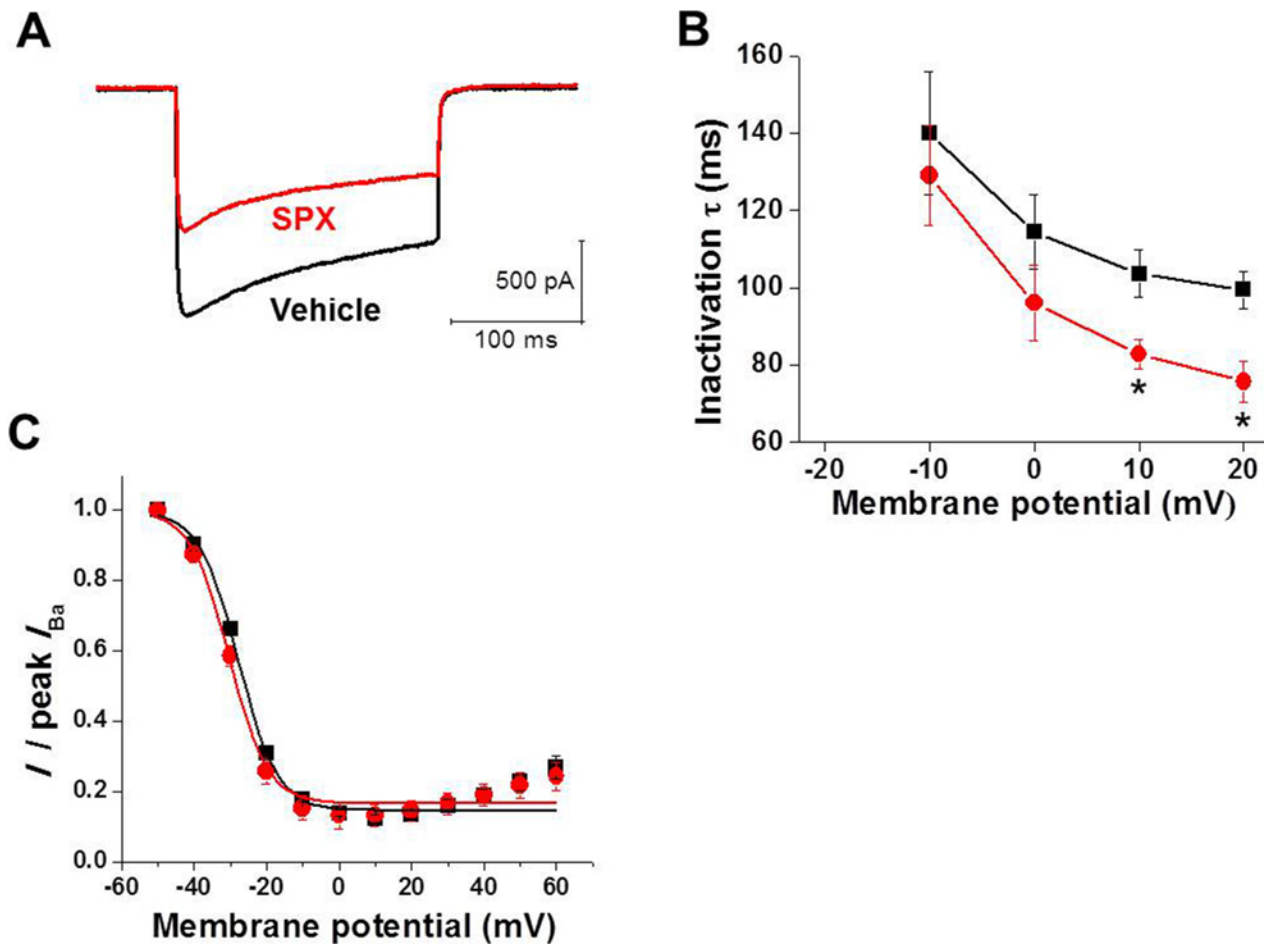
Fig 5. Effects of SPX on Ba^{2+} currents. A, Representative traces of I_{CaL} with external Ba^{2+} replacing Ca^{2+} as charge carrier during a 200 ms voltage-clamp pulse from –50 to 0 mV before (black) and after (red) exposure to 300 μM SPX. B, Voltage-dependence of Ba^{2+} current inactivation time constants (τ) under control conditions (black) and in the presence of 300 μM SPX (red). Data points (mean ± standard error) are from 5 cells. C, The steady-state inactivation curves of Ba^{2+} currents under control conditions (black) and in the presence of 300 μM SPX (red) (n = 3). *P < 0.05.

doi:10.1371/journal.pone.0149198.g005

Recovery from inactivation

Inactivation and recovery from inactivation are closely related processes and are critical factors that determine channel function. Recovery from inactivation was investigated by eliciting sustained depolarization (200 ms), followed by recovery intervals of increasing durations, and then applying a subsequent test pulse (Fig 7A, inset). In comparison to the control, recovery from inactivation was not changed by SPX treatment (Fig 7A and 7B). Data were fitted to a single exponential function. The time constants for recovery from inactivation were 365.4 ± 20.0 ms (n = 7) in the control and 382.6 ± 22.9 ms (n = 7) in the presence of SPX (paired *t*-test, P > 0.05).

Effect of SPX on I_{CaL} and AP in adult mouse cardiac myocytes

We then examined whether SPX still increases late I_{CaL} and APDs in cardiac myocytes from adult mouse (6 month old), which is lack of native I_{Kr}. We performed experiments similar to that shown in Fig 2. Fig 8A and 8C show that late I_{CaL} in adult mouse ventricular myocytes was significantly increased by exposure to 300 μM SPX for 10 min. Interestingly, SPX-induced
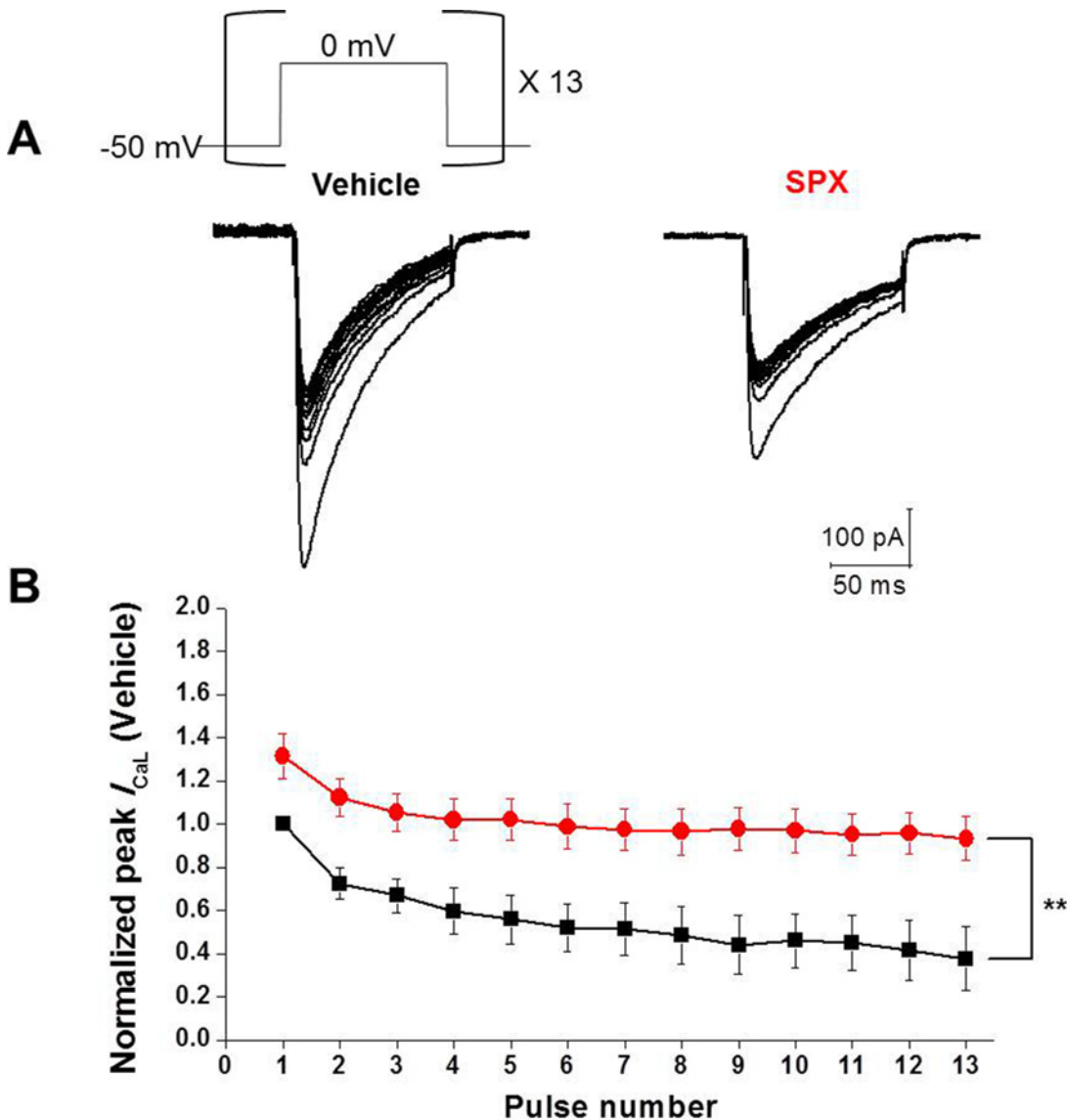
Fig 6. Use-dependency of SPX on I_{CaL}. A, Repetitive application of depolarizing pulses (shape is shown in the figure inset) to 0 mV from a holding potential of –50 mV gradually decreased the I_{CaL} amplitude. The frequency of depolarizing pulses was 2 Hz. In the presence of SPX, the gradual decrease of I_{CaL} was significantly attenuated. B, Summary of the use-dependent effect of SPX. Normalized current levels are plotted against pulse number (A and B, n = 6; black, control; red, SPX). The amplitudes of steady-state currents of both control and SPX group were normalized by the first current of the control. *P < 0.05 **P < 0.01 (n = 6).

doi:10.1371/journal.pone.0149198.g006

reduction of peak I_{CaL} in adult mouse ventricular myocytes was not so pronounced as that observed in neonatal cardiac myocytes (Fig 8B). Consistent with increase in late I_{CaL}, AP prolongation was observed when adult mouse cardiac myocytes were treated with SPX (300 μM) (Fig 8D & 8E). Fig 8E summarizes these results and shows that SPX prolonged APD_{90} over a range of stimulation rate in adult mouse cardiomyocytes. In addition, with exposure to SPX, triggered beats arising from early and delayed afterdepolarizations were observed in all cardiac myocytes examined at slow stimulation rate (n = 4); an example is shown in Fig 8F. In the absence of drug exposure, no afterdepolarizations were observed in cells (n = 4, Fig 8G). These findings exclude the potential E4031 effect and support the idea that SPX can increase late I_{CaL}
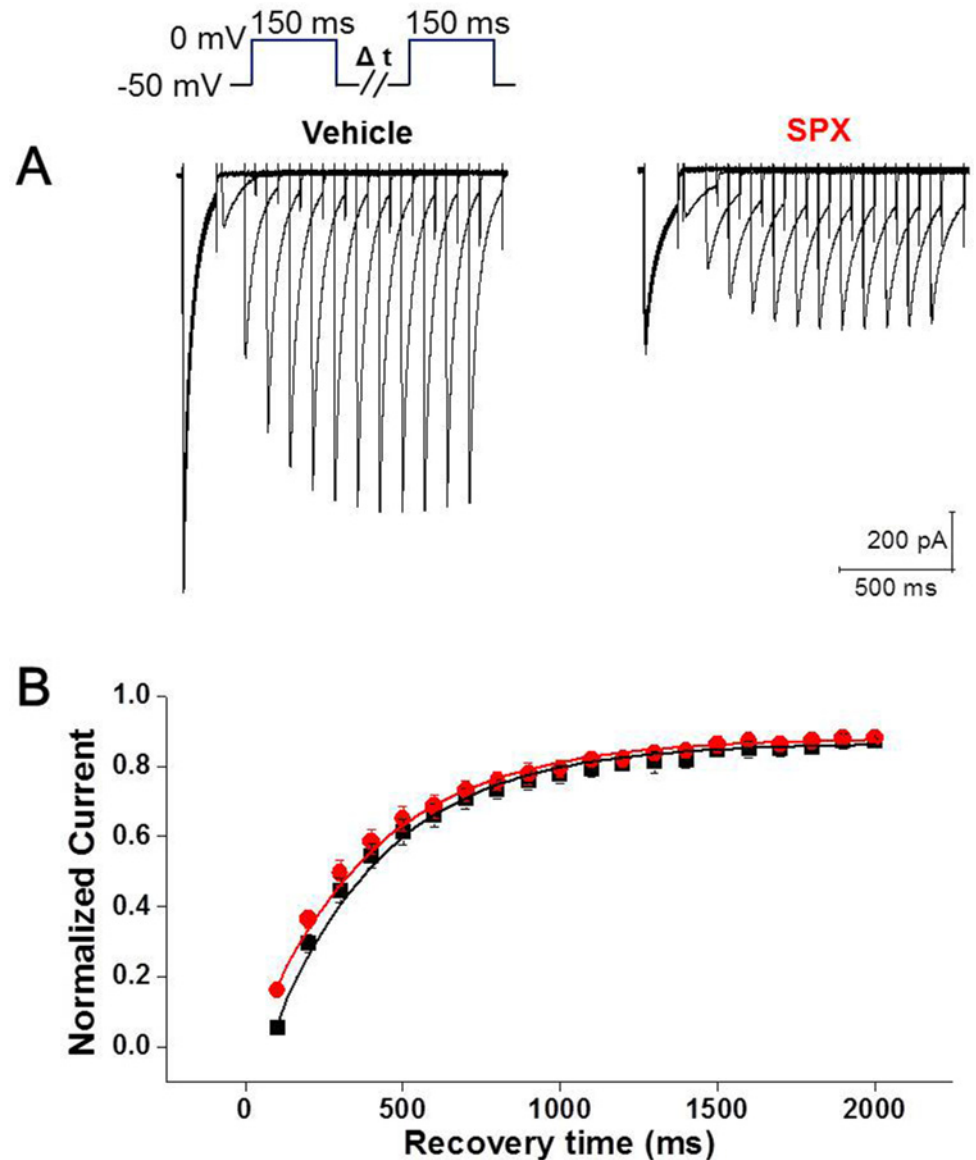
Fig 7. Effect of SPX on time course of the recovery from inactivation. A, Raw current tracings in the absence and presence of SPX. The voltage pulse protocol is shown as a figure inset. B, Summary of time courses of the recovery from inactivation in the absence and presence of SPX ($n = 6$; black, vehicle; red, SPX). *$P < 0.05$ **$P < 0.01$.

doi:10.1371/journal.pone.0149198.g007

and APDs in cardiac myocytes. Recently it was demonstrated that chronic exposure to some I_{Kr} blockers also increases cardiac late Na^+ current, which is probably regarded as another mechanism for the drug-induced Q-T prolongation and TdP in patients chronically exposed to (non)-cardiac drugs in clinics [19]. We examined whether chronic exposure (5 hrs) to SPX enhances late Na^+ currents in adult mouse ventricular myocytes. However no differences in late Na^+ currents were observed between control and SPX-treated cells (S3 Fig), suggesting that the SPX effect on APs could not be attributed to a change in late Na^+ currents.
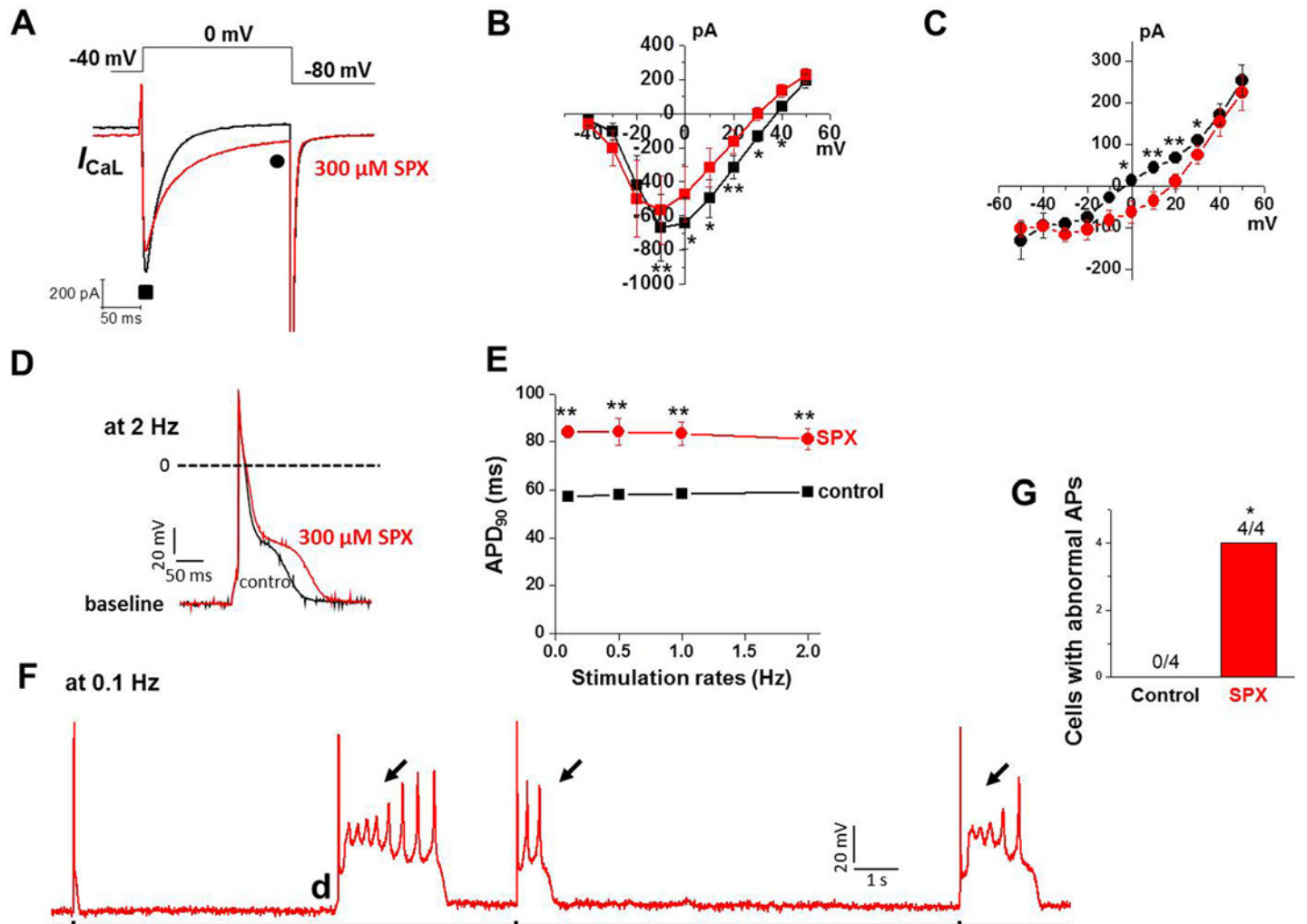
Fig 8. Effect of SPX on I_{CaL} and AP in adult mouse cardiac myocytes. A, Representative traces of I_{CaL} during a 200-ms voltage-clamp pulse from –40 to 0 mV before (black) and after (red) exposure to 300 µM SPX. B–C, current–voltage (I-V) relationships of I_{peak} (■, B) and $I_{end\ of\ pulse}$ (●, C) under control conditions (black) and after application of 300 µM SPX (red) (n = 4). D. SPX prolonged APs of adult mouse cardiomyocyte at a stimulation rate of 2 Hz. E, Plot of APD$_{90}$ over a range of stimulation rate in adult mouse cardiomyocytes in the absence and presence of SPX. F. Example of AP recorded after 30 min exposure to SPX at a slow stimulation rate (0.1 Hz). EADs (arrows) and delayed afterdepolarization (DAD; d) were observed, G. Summary data showing frequency of afterdepolarizations in control and SPX-treated cells. Incidence of EAD or DAD was analyzed using Fisher's exact test. *$P < 0.05$, **$P < 0.01$.

doi:10.1371/journal.pone.0149198.g008

Discussion

It has been argued that the extent of I_{Kr} block is imperfect at best as a predictor of effects of a drug in a human subject [20, 21]. Proposed reasons for this discrepancy include a time-dependent effect on biosynthesis of hERG channel or on cell surface trafficking [22, 23] or failure of in vitro testing to consider other ion channel actions such as I_{CaL} or late Na$^+$ currents [19, 24]. Our data showed that SPX markedly prolonged APD in a concentration-dependent manner in cardiac myocytes that lack I_{Kr}, suggesting that SPX can be arrhthmogenic via an I_{Kr}-independent pathway. SPX reduced peak I_{CaL} but augmented late I_{CaL} recorded several hundred milliseconds after a step depolarization and thus associated with APD prolongation. This effect is not seen with I_{Kr} blockers not associated with severe arrhythmias (ciprofloxacin, enoxacin, ofloxacin, and levofloxacin). We further showed that an antifungal agent ketoconazole, a potent I_{Kr} blocker without severe arrhythmias reduced both peak and late I_{CaL}, suggesting a

close relationship between late I_{CaL} and arrhythmogenesity. Detailed analysis showed that SPX treatment reduced the Ca^{2+}-dependent component of steady-state inactivation, indicating that SPX attenuated CDI. Consequently, the steady-state levels of I_{CaL} were increased in the presence of SPX compared to that of the control. Consistent with the observed SPX-induced CDI attenuation, SPX had little effect on the inactivation time constant and steady-state inactivation once extracellular Ca^{2+} was replaced with Ba^{2+}, a scenario in which essentially all inactivation is voltage dependent. The progressive use-dependent decrease of I_{CaL}, which was assessed by applying repetitive voltage pulses at 2Hz, was less pronounced in the presence of SPX, indicating the positive effect of SPX on I_{CaL} occurred in a use-dependent manner. The recovery from inactivation of I_{CaL} was not altered by SPX. Taken together, our data suggest that SPX attenuates CDI, and the resulting slower I_{CaL} decay might contribute to SPX-associated EAD and TdP.

The positive effects of SPX on I_{CaL} were concentration dependent, and SPX started to slow Ca^{2+} channel inactivation at a treatment concentration of 10 μM (Fig 3). Moreover, SPX-induced APD prolongation in the presence of E4031 was evident at 30 μM (Fig 1). Because the steady-state plasma concentration of SPX in healthy volunteers and patients was 1.8 μM and the hERG IC$_{50}$ value is 18 μM [16], these results suggest that the slowing of I_{CaL} inactivation may attributable to SPX-induced LQT or arrhythmia under clinical conditions.

We demonstrated that SPX attenuated late I_{CaL} inactivation, especially at depolarized potentials ($\geq$0 mV) without voltage shift of steady-state curve. Therefore, inactivation curve was more U-shaped in the presence of SPX (Fig 4). These results suggest that SPX specifically interrupts the Ca^{2+}-dependent component of I_{CaL} inactivation, having little effect on the voltage-dependent component. In support of this hypothesis, when Ba^{2+} was used as the I_{CaL} charge carrier (Fig 5), SPX-induced inactivation slowing and the consequent increase in the late I_{CaL} were abolished (Fig 5).

Our data showed that SPX treatment reduced peak I_{CaL} amplitude as well as slowed its inactivation. These two changes have opposing effects on APD. However, the results of previous studies suggest that the kinetics of I_{CaL} inactivation, rather than the amplitude modulates its effects on the APD restitution slope and reentry [25]. Consistent with this concept, SPX induced APD prolongation, because of the dominance of suppressed I_{CaL} inactivation in controlling APD compared to the ongoing reduction of I_{CaL} amplitude. In a context in which there is a concomitant reduction of repolarizing current, which should shorten APs, the slowed I_{CaL} decay is an important factor in tipping the balance towards EAD formation.

Although the precise molecular sites that are responsible for the CDI is not entirely clear yet, it has been demonstrated that two kinds of Ca^{2+}-binding sites model (i.e., high-affinity slow and low-affinity fast kinetic binding sites) successfully simulated the CDI obtained by experiments [26, 27]. The high affinity binding site was expected to be present very near at inner channel mouth and not to be accessible by intracellular Ca^{2+} buffers such as EGTA or BPATA. Therefore, this CDI is attributable by the influx of Ca^{2+} itself and can't be excluded by pipette EGTA or BAPTA. It can only be excluded by the substitution of Ca^{2+} with other ions such as Ba^{2+} for the charge carrier. Classically, the 'domain' model of CDI can explain well this high affinity Ca^{2+} binding site model [26–28]. The low-affinity Ca^{2+} binding site can explain well the 'shell' model of CDI, in which global increase in cytosolic [Ca^{2+}]i mediates the CDI [27, 28]. The Ca^{2+} that are released from intracellular store such as sarcoplasmic reticulum (SR) took the biggest part in the 'shell' or 'low-affinity Ca^{2+} binding site' models [27]. Therefore, the release-dependent inactivation (RDI) was primarily responsible for CDI in the 'low-affinity Ca^{2+} binding site' model [27]. High concentrations of pipette Ca^{2+} buffer such as BAPTA can effectively exclude this CDI that is mediated by the low-affinity Ca^{2+} binding site. Since we used pipette solution with 10 mM EGTA in the present study, it is expected that SR

Ca^{2+} is depleted and the CICR is largely prevented. Therefore, the CDI of this study is thought to be primarily mediated by the high affinity Ca^{2+} binding site probably very near at the channel mouth. Taken together, the slowing of inactivation time course of I_{CaL} by SPX was not secondary phenomenon due to the decreases in peak I_{CaL} and intracellular [Ca^{2+}], but due to SPX-induced specific inhibition of CDI that is mediated by high affinity Ca^{2+}-binding site (that is, an EGTA-insensitive site). Moreover, lack of effects on the inactivation time courses by ketoconazole (Fig 2), at concentrations that inhibit the peak I_{CaL} similarly to those of SPX, also indicates that the CDI of the present study is not mediated by the global intracellular [Ca^{2+}] increase.

In conclusion, the present findings demonstrate the role of I_{CaL} in SPX-induced APD prolongation. Our results suggest that modification of I_{CaL} properties, in addition to I_{Kr} antagonistic activities, should be considered when assessing the proarrhythmic potential of drugs. Especially new drug evaluation will need to look beyond effect on peak I_{CaL} and examine drug effects on late I_{CaL} of which perturbation induces abnormal repolarization.

Supporting Information

S1 Fig. L-type and T-type Ca^{2+} channels in neonatal rat cardiomyocytes A, Ca^{2+} currents were elicited by depolarizing voltage steps from a holding potential of −80 mV in the absence and presence of nifedipine (1 μM) or nifedipine (1 μM) plus NiCl$_2$ (100 μM). B, Current–voltage (I–V) relationships of the peak Ca^{2+} current (holding potential −80 mV) in the absence and presence of Ca^{2+} channel inhibitors (black, control; red, Nifedipine; green, Nifedipine + NiCl$_2$. C, Ca^{2+} currents were elicited by depolarizing voltage steps from a holding potential of −50 mV in the absence and presence of nifedipine (1 μM). D, Current–voltage (I–V) relationships of the peak Ca^{2+} currents in the absence and presence of nifedipine (holding potential −50 mV; black, control; red, nifedipine).
(TIF)

S2 Fig. Effects of quinolones on I_{CaL} Representative traces showing the effect of 1 mM ciprofloxacin (A), 1 mM enoxacin (B), 1 mM ofloxacin (C), and 1 mM levofloxacin (D) on I_{CaL}. Representative traces of I_{CaL} during a 200-ms voltage-clamp pulse from −40 to 0 mV before (black) and after (red) exposure to 300 μM SPX. Lower panels (E–H) summarize the concentration-response of the quinolones.
(TIF)

S3 Fig. Chronic exposure to SPX does not increase late Na$^+$ current A, Examples of Na$^+$ current recorded 5 hours after isolation in the absence (vehicle; left), or in the presence of SPX (right). The selective late current blocker ranolazine did not affect Na$^+$ current in SPX-treated cells as well as cells under control condition. B, Summary data show that there was no effect on late Na$^+$ current of 5-hour exposure to SPX in adult mouse ventricular myocytes.
(TIF)

Author Contributions

Conceived and designed the experiments: BK HCS HC YMB. Performed the experiments: JGK DJS SWP HK KJW. Analyzed the data: JGK CHL YHZ KSK. Wrote the paper: HC YMB.

References

1. Cubeddu LX. QT prolongation and fatal arrhythmias: a review of clinical implications and effects of drugs. Am J Ther. 2003; 10(6):452–7. PMID: 14624285.

2. Raehl CL, Patel AK, LeRoy M. Drug-induced torsade de pointes. Clin Pharm. 1985; 4(6):675–90. PMID: 2416504.

3. Shah RR. Pharmacogenetic aspects of drug-induced torsade de pointes: potential tool for improving clinical drug development and prescribing. Drug Saf. 2004; 27(3):145–72. PMID: 14756578.

4. Viskin S, Justo D, Halkin A, Zeltser D. Long QT syndrome caused by noncardiac drugs. Prog Cardiovasc Dis. 2003; 45(5):415–27. doi: 10.1053/pcad.2003.00101 PMID: 12704598.

5. Olsen KM. Pharmacologic agents associated with QT interval prolongation. J Fam Pract. 2005;Suppl: : S8–S14. PMID: 15938993.

6. Psaty BM. Clinical trial design and selected drug safety issues for antibiotics used to treat community-acquired pneumonia. Clin Infect Dis. 2008; 47 Suppl 3:S176–9. doi: 10.1086/591400 PMID: 18986285; PubMed Central PMCID: PMCPMC2587028.

7. Anderson ME, Mazur A, Yang T, Roden DM. Potassium current antagonist properties and proarrhythmic consequences of quinolone antibiotics. J Pharmacol Exp Ther. 2001; 296(3):806–10. PMID: 11181910.

8. Bloomfield DM, Kost JT, Ghosh K, Hreniuk D, Hickey LA, Guitierrez MJ, et al. The effect of moxifloxacin on QTc and implications for the design of thorough QT studies. Clin Pharmacol Ther. 2008; 84(4):475–80. PMID: 19238652.

9. Dale KM, Lertsburapa K, Kluger J, White CM. Moxifloxacin and torsade de pointes. Ann Pharmacother. 2007; 41(2):336–40. doi: 10.1345/aph.1H474 PMID: 17284508.

10. Xu X, Yan GX, Wu Y, Liu T, Kowey PR. Electrophysiologic effects of SB-237376: a new antiarrhythmic compound with dual potassium and calcium channel blocking action. J Cardiovasc Pharmacol. 2003; 41(3):414–21. PMID: 12605020.

11. Alseikhan BA, DeMaria CD, Colecraft HM, Yue DT. Engineered calmodulins reveal the unexpected eminence of Ca2+ channel inactivation in controlling heart excitation. Proc Natl Acad Sci U S A. 2002; 99(26):17185–90. doi: 10.1073/pnas.262372999 PMID: 12486220; PubMed Central PMCID: PMCPMC139290.

12. Sung DJ, Kim JG, Won KJ, Kim B, Shin HC, Park JY, et al. Blockade of K+ and Ca2+ channels by azole antifungal agents in neonatal rat ventricular myocytes. Biol Pharm Bull. 2012; 35(9):1469–75. PMID: 22975497.

13. Yoon JY, Ahn SH, Oh H, Kim YS, Ryu SY, Ho WK, et al. A novel Na+ channel agonist, dimethyl lithospermate B, slows Na+ current inactivation and increases action potential duration in isolated rat ventricular myocytes. Br J Pharmacol. 2004; 143(6):765–73. doi: 10.1038/sj.bjp.0705969 PMID: 15504759; PubMed Central PMCID: PMCPMC1575928.

14. Hille B. Ion channels of excitable membranes. 3rd ed. Sunderland, Mass.: Sinauer; 2001. xviii, 814 p. p.

15. Frothingham R. Rates of torsades de pointes associated with ciprofloxacin, ofloxacin, levofloxacin, gatifloxacin, and moxifloxacin. Pharmacotherapy. 2001; 21(12):1468–72. PMID: 11765299.

16. Kang J, Wang L, Chen XL, Triggle DJ, Rampe D. Interactions of a series of fluoroquinolone antibacterial drugs with the human cardiac K+ channel HERG. Mol Pharmacol. 2001; 59(1):122–6. PMID: 11125032.

17. Tsai WC, Tsai LM, Chen JH. Combined use of astemizole and ketoconazole resulting in torsade de pointes. J Formos Med Assoc. 1997; 96(2):144–6. PMID: 9071844.

18. Zimmermann M, Duruz H, Guinand O, Broccard O, Levy P, Lacatis D, et al. Torsades de Pointes after treatment with terfenadine and ketoconazole. Eur Heart J. 1992; 13(7):1002–3. PMID: 1644069.

19. Yang T, Chun YW, Stroud DM, Mosley JD, Knollmann BC, Hong C, et al. Screening for acute IKr block is insufficient to detect torsades de pointes liability: role of late sodium current. Circulation. 2014; 130 (3):224–34. doi: 10.1161/CIRCULATIONAHA.113.007765 PMID: 24895457; PubMed Central PMCID: PMCPMC4101031.

20. Hoffmann P, Warner B. Are hERG channel inhibition and QT interval prolongation all there is in drug-induced torsadogenesis? A review of emerging trends. J Pharmacol Toxicol Methods. 2006; 53(2):87–105. doi: 10.1016/j.vascn.2005.07.003 PMID: 16289936.

21. Lu HR, Vlaminckx E, Hermans AN, Rohrbacher J, Van Ammel K, Towart R, et al. Predicting drug-induced changes in QT interval and arrhythmias: QT-shortening drugs point to gaps in the ICHS7B Guidelines. Br J Pharmacol. 2008; 154(7):1427–38. doi: 10.1038/bjp.2008.191 PMID: 18493243; PubMed Central PMCID: PMCPMC2440085.

22. Ficker E, Kuryshev YA, Dennis AT, Obejero-Paz C, Wang L, Hawryluk P, et al. Mechanisms of arsenic-induced prolongation of cardiac repolarization. Mol Pharmacol. 2004; 66(1):33–44. doi: 10.1124/mol.66.1.33 PMID: 15213294.

23. Kuryshev YA, Ficker E, Wang L, Hawryluk P, Dennis AT, Wible BA, et al. Pentamidine-induced long QT syndrome and block of hERG trafficking. J Pharmacol Exp Ther. 2005; 312(1):316–23. doi: 10.1124/jpet.104.073692 PMID: 15340016.

24. Kuryshev YA, Wang L, Wible BA, Wan X, Ficker E. Antimony-based antileishmanial compounds prolong the cardiac action potential by an increase in cardiac calcium currents. Mol Pharmacol. 2006; 69 (4):1216–25. doi: 10.1124/mol.105.019281 PMID: 16418337.

25. Mahajan A, Sato D, Shiferaw Y, Baher A, Xie LH, Peralta R, et al. Modifying L-type calcium current kinetics: consequences for cardiac excitation and arrhythmia dynamics. Biophys J. 2008; 94(2):411–23. doi: 10.1529/biophysj.106.98590 PMID: 18160661; PubMed Central PMCID: PMCPMC2157257.

26. Markevich NI, Pimenov OY, Kokoz YM. Analysis of the modal hypothesis of Ca2+-dependent inactivation of L-type Ca2+ channels. Biophys Chem. 2005; 117(2):173–90. doi: 10.1016/j.bpc.2005.04.017 PMID: 15936868.

27. Ryu JS, Kim WT, Lee JH, Kwon JH, Kim HA, Shim EB, et al. Analysis of factors affecting Ca(2+)-dependent inactivation dynamics of L-type Ca(2+) current of cardiac myocytes in pulmonary vein of rabbit. J Physiol. 2012; 590(Pt 18):4447–63. doi: 10.1113/jphysiol.2012.229203 PMID: 22674726; PubMed Central PMCID: PMCPMC3477751.

28. Budde T, Meuth S, Pape HC. Calcium-dependent inactivation of neuronal calcium channels. Nat Rev Neurosci. 2002; 3(11):873–83. doi: 10.1038/nrn959 PMID: 12415295.